

# Multi-modal Image Registration Using the Generalized Survival Exponential Entropy

Shu Liao and Albert C.S. Chung

Lo Kwee-Seong Medical Image Analysis Laboratory,  
Department of Computer Science and Engineering,  
The Hong Kong University of Science and Technology, Hong Kong  
liaoshu@cse.ust.hk, achung@cse.ust.hk

**Abstract.** This paper introduces a new similarity measure for multi-modal image registration task. The measure is based on the generalized survival exponential entropy (GSEE) and mutual information (GSEE-MI). Since GSEE is estimated from the cumulative distribution function instead of the density function, it is observed that the interpolation artifact is reduced. The method has been tested on four real MR-CT data sets. The experimental results show that the GSEE-MI-based method is more robust than the conventional MI-based method. The accuracy is comparable for both methods.

## 1 Introduction

Image registration has been an important issue in medical image analysis. Given multiple registered images, the complementary and useful image information obtained from different modalities can be combined. The goal of image registration is to estimate a geometric transformation such that two medical images can be aligned accurately. Mutual information (MI) has been used widely as a similarity measure for multi-modal image registration tasks [1,2,3]. In this paper, we introduce the use of generalized survival exponential entropy (GSEE) for estimation of mutual information (GSEE-MI) in image registration, and compare the performance between MI and GSEE-MI in terms of robustness and accuracy.

The GSEE-MI-based image registration method utilizes the generalized survival exponential entropy, which is estimated from the cumulative distribution function instead of the density function. In some real-world applications, the cumulative distribution function is more natural than the density function because it is defined in integral form, which can give more reliable estimation (i.e., it always exists even when the density function does not exist [4]).

The GSEE-MI-based method has been tested on four MR-CT data sets obtained from the Retrospective Image Registration Evaluation project. The performance of GSEE-MI has been examined along the translation (X-, Y- and Z-axis) and rotation axes. It is observed that the values of GSEE-MI decrease smoothly from the optimal transformation. Moreover, because of the use of cumulative distribution function, the interpolation artifact is reduced in the GSEE-MI-based method. These factors can improve the robustness of an image registration

method. It is experimentally shown that the GSEE-MI-based method is more robust than the conventional MI-based method. The accuracy of both methods is comparable.

## 2 Methodology

### 2.1 Joint Intensity Distribution Acquisition

Let  $G_f$  and  $G_r$  be the floating and reference images respectively, which are obtained from the same or different acquisitions. Assume that  $I_f$  and  $I_r$  represent their intensity values,  $X_f$  and  $X_r$  are their image domains. With a hypothesized transformation  $T$ , samples of intensity pairs  $I = \{i_r(x), i_f(T(x)) \mid i_r \in I_r, i_f \in I_f\}$  can be drawn randomly from  $I_f$  and  $I_r$ , where  $x$  are the pixel coordinates,  $x \in \Omega$  and  $\Omega \subset X_f \cup X_r$ . That is, the sampling domain is inside  $X_f \cup X_r$ .

The joint intensity distribution is denoted as  $P^T(I_r, I_f)$ . It depends on the specific hypothesized transformation  $T$  and changes during the registration process. There are two methods to approximate  $P^T(I_r, I_f)$ : the Parzen windowing or histogramming [5]. This paper employs histogramming as it is more computationally efficient. The bin size of the histogram is set to 32 in this paper. The histogram partial volume (PV) interpolation method is employed [6].

### 2.2 Generalized Survival Exponential Entropy: A New Measure of Information

In this section, the Survival Exponential Entropy (SEE) and the Generalized Survival Exponential Entropy (GSEE) [7] are introduced. GSEE is a new information measurement of random variables. Their definitions are given as follows:

*Definition 1:* For a random vector  $X$  in  $R^m$ , the survival exponential entropy of order  $\alpha$  is [7]:

$$M_\alpha(X) = \left( \int_{R^m_+} \overline{F}_{|X|}^\alpha(x) dx \right)^{\frac{1}{1-\alpha}} \tag{1}$$

for  $\alpha \geq 0$ , where  $m$  defines the number of dimensions for  $X$ .

*Definition 2:* For a random vector  $X$  in  $R^m$ , the generalized survival exponential entropy of order  $(\alpha, \beta)$  is [7]:

$$S_{\alpha,\beta}(X) = \left( \frac{\int_{R^m_+} \overline{F}_{|X|}^\alpha(x) dx}{\int_{R^m_+} \overline{F}_{|X|}^\beta(x) dx} \right)^{\frac{1}{\beta-\alpha}} \tag{2}$$

for  $\alpha, \beta \geq 0$  and  $\alpha \neq \beta$ , where  $X = (X_1, \dots, X_m)$  is a random vector in  $R^m$ .  $|X|$  denotes the random vector with components  $|X_1|, \dots, |X_m|$ . The notation

$|X| > x$  means that  $|X_i| > x_i$  for  $x_i \geq 0, i = 1, \dots, m$ . The multivariate survival function  $\overline{F}_{|X|}(x)$  of the random vector  $|X|$  is defined by:

$$\overline{F}_{|X|}(x) = P(|X| > x) = P(|X_1| > x_1, \dots, |X_m| > x_m) \tag{3}$$

for  $x \in R_+^m$  with  $R_+^m = \{x \in R^m : x = (x_1, \dots, x_m), x_i \geq 0, i = 1, \dots, m\}$ .

Compare to the conventional information measurement of Shannon’s entropy,  $H(X)$ , SEE and GSEE replace the density function with the cumulative distribution in Shannon’s definition [8]. The distribution function actually is more regular than the density function in that it is defined in the integral form. The density function is the derivative of the distribution. The extension of the Shannon’s Entropy to the continuous distribution is called the differential entropy [4]. The SEE and GSEE have several advantages over the Shannon entropy and differential entropy: (1) SEE and GSEE have consistent definitions in both the continuous and discrete domains; (2) SEE and GSEE are always nonnegative; (3) SEE and GSEE are easy to compute from sample data; (4) The Shannon’s Entropy is based on the density of the random variable  $p(X)$ . As pointed out by [9], in general,  $p(X)$  may not exist [9] [4]. Even if it exists, it also needs to be estimated. The estimated value of  $p(X)$  converges to the true density only under some conditions [4].

For the applications in image registration, the SEE-based Mutual Information (SEE-MI) and the GSEE-based Mutual Information (GSEE-MI) are introduced. The mutual information (MI) similarity measure of images  $G_r$  and  $G_f$ :  $I(G_r, T(G_f))$  using Shannon entropy is defined as [6]:

$$I(G_r, T(G_f)) = H(p(G_r)) - E[H(p(G_r))/p(T(G_f))] \tag{4}$$

where  $p(G_r)$  and  $p(T(G_f))$  are the marginal distributions of the probability distribution histogram of the reference image and the floating image respectively. The conventional MI measure suffered from the drawbacks of the Shannon’s Entropy mentioned before. To overcome such shortage, SEE-MI and GSEE-MI are introduced as follows:

$$\text{SEE-MI}(G_r, T(G_f)) = M_\alpha(p(G_r)) - E[M_\alpha(p(T(G_f))/p(G_r))], \tag{5}$$

for  $\alpha \geq 0$ .

$$\text{GSEE-MI}(G_r, T(G_f)) = S_{\alpha,\beta}(p(G_r)) - E[S_{\alpha,\beta}(p(T(G_f))/p(G_r))], \tag{6}$$

for  $\alpha, \beta \geq 0$  and  $\alpha \neq \beta$ , where  $M_\alpha(p(T(G_f))/p(G_r))$  and  $S_{\alpha,\beta}(p(T(G_f))/p(G_r))$  are the conditional SEE and GSEE, the conditional SEE and GSEE are defined as [7]:

$$M_\alpha(X | Y) = \left( \int_0^\infty \overline{F}_{X|Y}^\alpha(x | y) dx \right)^{\frac{1}{1-\alpha}} \tag{7}$$

for  $\alpha \geq 0$ , and

$$S_{\alpha,\beta}(X | Y) = \left( \frac{\int_0^{\infty} \overline{F}_{X|Y}^{\alpha}(x | y) dx}{\int_0^{\infty} \overline{F}_{X|Y}^{\beta}(x | y) dx} \right)^{\frac{1}{\beta-\alpha}} \quad (8)$$

for  $\alpha, \beta \geq 0$  and  $\alpha \neq \beta$ .

### 2.3 Optimization of SEE-MI and GSEE-MI

Given definitions of SEE-MI and GSEE-MI in Equations 5 and 6, the goal of the registration is to find the optimal transformation  $\hat{T}$  by maximizing the SEE-MI or GSEE-MI values, which is formulated as:

$$\hat{T} = \arg \max_T \text{SEE-MI}(G_r, T(G_f)) \quad (9)$$

for  $\alpha \geq 0$ , and

$$\hat{T} = \arg \max_T \text{GSEE-MI}(G_r, T(G_f)) \quad (10)$$

for  $\alpha, \beta \geq 0$  and  $\alpha \neq \beta$ .

The proposed method is an unsupervised registration method which does not need any pre-aligned training pairs in advanced. In this paper, only GSEE-MI is used in the experiments as it is more general than SEE-MI and more flexible because GSEE-MI has two parameters  $\alpha$  and  $\beta$  for the maximization of mutual information. The value of GSEE-MI is maximized using the Powell's method [10]. The Powell's method searches for the maximum value of GSEE-MI iteratively along each parameter axis  $T$  while others are kept constant. The search step  $\partial T$  is set to 0.02 mm for the translation parameters along  $X$ ,  $Y$  and  $Z$  axis and 0.2 degree for the rotation parameters about  $X$ ,  $Y$  and  $Z$  axis. During each iteration of the Powell's method, the *grid search* is performed to search the optimal pair of  $\alpha$  and  $\beta$  in the range from  $2^{-5}$  to  $2^5$  with step size  $2^{\frac{1}{4}}$  in order to maximize the value of GSEE-MI. The iterative search process stops when the value of GSEE-MI is converged (i.e., when the change of GSEE-MI is sufficiently small, it is set to be 0.001 in this paper).

## 3 Experimental Results

### 3.1 Probing Performance of MR-CT(3D-3D) Registration

Four pairs of CT and MR image volumes are obtained from the Retrospective Image Registration Evaluation project<sup>1</sup>. One of the pairs of 2D CT and MR image slices is shown in Figure 1.

We chose the CT images as the reference image  $G_r$  and the MR images as the floating images  $G_f$ . In order to study the performance of the objective function,

<sup>1</sup> The images were provided as part of the project, "Retrospective Image Registration Evaluation", National Institutes of Health, Project Number 8R01EB002124-03, Principal Investigator, J. Michael Fitzpatrick, Vanderbilt University, Nashville, TN.

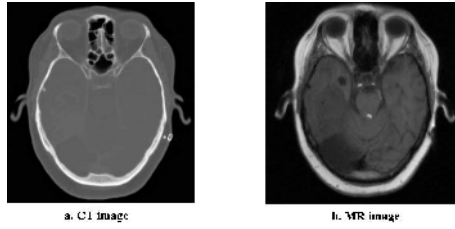


Fig. 1. One pair of 2D CT and MR image slices

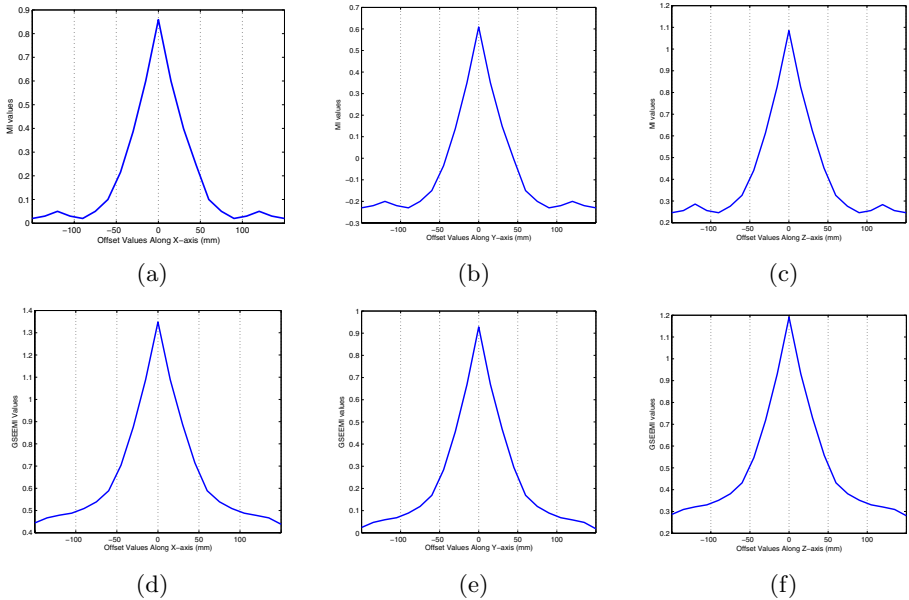
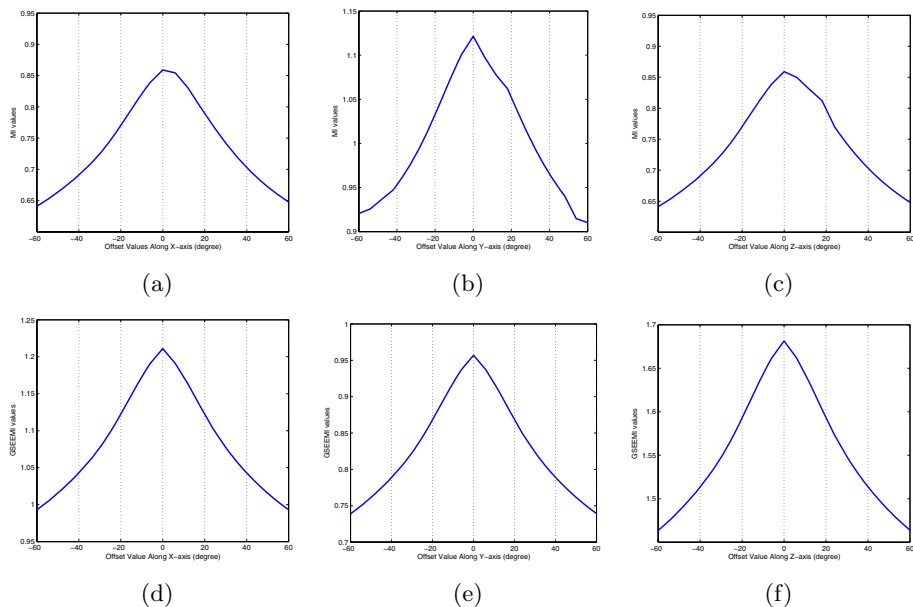


Fig. 2. MI: Shifting Probes Along (a) X-axis and (b) Y-axis and (c) Z-axis; GSEE-MI: Shifting Probes Along (d) X-axis and (e) Y-axis and (f) Z-axis

$G_f$  was shifted along and rotated about the  $X$ ,  $Y$  and  $Z$  axes while  $G_r$  were fixed. For a specific transformation  $T$ , if a pixel  $x_i$  of  $G_f$  fell between the voxel positions of  $G_r$ , then the PV interpolation [6] was applied to achieve subvoxel accuracy. Figure 2 plots the translational probes of shifting along three axes for MI and GSEE-MI respectively. Figure 3 plots the rotational probes for MI and GSEE-MI respectively.

As shown in Figure 2, for the conventional MI measure, there are obvious local maxima when the misalignment of two images is relatively large (i.e., floating image is shifted from  $-100$  to  $-200$  mm and  $100$  to  $200$  mm along  $X$ ,  $Y$  and  $Z$  axes). The main reason is that the estimation of density function of the Shannon’ Entropy used in the conventional MI does not converge to the true density in such case. However, from Figure 2, it is observed that the probing curves based on GSEE-MI are improved as they do not have local maxima even when two



**Fig. 3.** MI: Rotational Probes About (a) X-axis and (b) Y-axis and (c) Z-axis; GSEE-MI: Rotational Probes About (d) X-axis and (e) Y-axis and (f) Z-axis

images have large misalignment because the density function is replaced by the distribution function. Therefore, the robustness of the GSEE-MI approach is greatly implied.

From the rotational probing curves (see Figure 3), we can see that although the MI curves do not have any local maxima, the GSEE-MI probing curves are smoother than the MI curves. Therefore, in such case, GSEE-MI performs more stable than the conventional MI measure.

To further demonstrate the robustness against the PV interpolation artifacts of the conventional MI and GSEE-MI similarity measures, the probing curves of the shifting range  $[-2, 2]$  mm for both methods are plotted in Figure 4, it implies that GSEE-MI is also more robust against the interpolation artifacts.

### 3.2 Registration Performance of MR-CT(3D-3D) Registration

To study and compare the registration robustness of the proposed GSEE-MI-based and the conventional MI-based image registration methods, a series of randomized experiments are designed to evaluate both methods. The testing images are the aforementioned four MR-CT pairs datasets (#1, #2, #3 and #4). For each pre-obtained ground truth registration MR-CT pair<sup>2</sup>, it was perturbed by six uniformly distributed random offsets for all translational and rotational axes.

<sup>2</sup> In the experiments, all registered pairs examined by the RIRE project. The median registration errors were all less than 1mm.

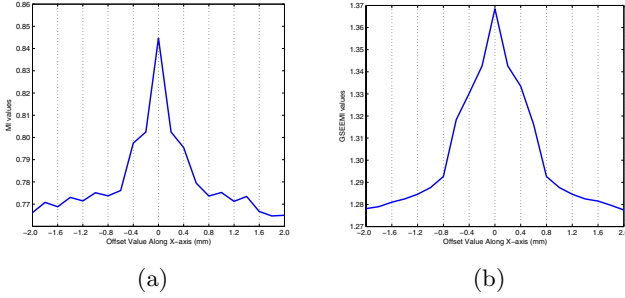


**Fig. 4.** (a) MI Translational Probes Along X-axis in the range  $[-2,2]$  mm; (b) GSEE-MI Translational Probes Along X-axis in the range  $[-2,2]$  mm

Then the perturbed registration image pair was used as the starting alignment. For each MR-CT pair, the experiment was repeated 100 times. The translational random offsets for  $X$  and  $Y$  axes were drawn between  $[-150,150]$  mm, the random offset for  $Z$  axis was drawn between  $[-70,70]$  mm. The rotational random offsets for  $X$ ,  $Y$  and  $Z$  axes were drawn between  $[-20,20]$  degrees. Also, for each MR-CT pair the same set or randomized starting alignment was used for both methods for fair comparison.

In the experiment, the translation errors (the root-sum-square of the differences for three translational axes) and the rotational errors (which was the real part of a quaternion) were computed. The threshold vector for assessing registration success was set to  $(2mm, 2^\circ)$  as registration errors below  $2mm$  and  $2^\circ$  are generally acceptable by experienced clinicians [11,12].

The success rate of the conventional MI approach and the proposed GSEE-MI approach is listed in Table 1. As we can see, the GSEE-MI approach has higher success rate than the conventional MI approach in each MR-CT pair dataset.

**Table 1.** Success rates of the conventional MI-based approach and the proposed GSEE-MI-based approach

Testing dataset	MI Success Rates	GSEE-MI Success Rates
#1	64%	95%
#2	63%	93%
#3	72%	97%
#4	65%	89%

To further precisely demonstrate the registration accuracy of the proposed method, the mean value and standard deviation of the registration errors in the successful registrations in all four MR-CT pairs for both MI and GSEE-MI methods are calculated and listed in Table 2. According to Table 2, the accuracies of the conventional MI approach and the proposed GSEE-MI approach for the successful registrations are comparable and acceptably high. However, we should

**Table 2.** Registration Accuracy of the conventional MI approach and the proposed GSEE-MI approach

Method	Translation ( $10^{-3}mm$ )			Rotation ( $10^{-3}degrees$ )		
	$\Delta t_x$	$\Delta t_y$	$\Delta t_z$	$\Delta \theta_x$	$\Delta \theta_y$	$\Delta \theta_z$
MI	$0.64 \pm 1.84$	$-0.37 \pm 0.73$	$1.16 \pm 1.32$	$0.85 \pm 1.84$	$-1.05 \pm 1.47$	$0.86 \pm 1.63$
GSEE-MI	$0.85 \pm 1.63$	$-0.62 \pm 0.34$	$1.05 \pm 1.57$	$1.32 \pm 0.62$	$-0.83 \pm 1.58$	$0.52 \pm 1.15$

bear in mind that the number of successful registrations of the GSEE-MI-based approach are significantly higher than that of the conventional MI-based method according to Table 1.

## 4 Conclusion

In this paper, we have proposed a new multi-modal image registration method using the generalized survival exponential entropy and mutual information (GSEE-MI). The experimental results show that the GSEE-MI-based method reduces the interpolation artifacts and is more robust than the conventional MI-based method. The future direction is to extend the current method and apply it to non-rigid image registration.

## References

1. Wells, W., Viola, P., et al.: Multi-Modal Volume Registration by Maximization of Mutual Information. *MedIA* **1**(1) (1996) 35–51
2. Maes, F., Collignon, A., et al.: Multimodality Image Registration by Maximization of Mutual Information. *TMI* **16**(2) (1997) 187–198
3. Pluim, J., Maintz, J., Viergever, M.: Mutual-information-based registration of medical images: a survey. *TMI* **22**(8) (2003) 986–1004
4. Cover, T.M., Thomas, J.A.: *Elements of Information Theory*. John Wiley and Sons (1991)
5. Bishop, C.: *Neural Networks for Pattern Recognition*. Oxford U. Press (1995)
6. Maes, F., Collignon, A., et al.: Multimodality Image Registration by Maximization of Mutual Information. *TMI* **16**(2) (1997) 187–198
7. Zografos, K., Nadarajah, S.: Survival Exponential Entropies. *IEEE Trans. on Information Theory* **51**(3) (2004) 1239–1246
8. Shannon, C.: A mathematical theory of communication. In: *Bell Syst. Tech. J. Volume 27*. (1948) 379–432
9. Wang, F., Vemuri, B., Rao, M., Chen, Y.: A New & Robust Information Theoretic Measure and its Application to Image Alignment. In: *The 18th IPMI*. (2003) 388–400
10. Press, W., Teukolsky, S., et al.: *Numerical Recipes in C*. Cambridge University Press (1992)
11. Hajnal, J.V., Hill, D.L.G., Hawkes, D.J.: *Medical Image Registration*. CRC Press LLC (2001)
12. Zhu, Y., Cochoff, S.: Likelihood Maximization Approach to Image Registration. *TIP* **11** (2002) 1417–1426